



Experimental research of the horizontal tube falling film flow patterns—transitional flow patterns and critical transition Re

Xingsen Mu^{a,*}, Shun Hu^a, Xiaowen Nie^a, Jiali Wu^b, Shanlin Liu^a, Shengqiang Shen^a

^aKey Laboratory of Ocean Energy Utilization and Energy Conservation of Ministry of Education, School of Energy and Power Engineering, Dalian University of Technology, Dalian 116024, China, email: muxingsen@dlut.edu.cn (X. Mu), 980789822@qq.com (S. Hu), 494719329@qq.com (X. Nie), liushanlin@dlut.edu.cn (S. Liu), zzbshen@dlut.edu.cn (S. Shen)

^bShenyang Normal University, email: luckyjiali@163.com (J. Wu)

Received 18 October 2021; Accepted 27 March 2022

ABSTRACT

The flow pattern of the fluid between the horizontal tubes is one of the important factors that affects the heat and mass transfer efficiency during the process of the horizontal tube falling film flow, and it is worthy of attention to optimize the performance of the horizontal tube falling film evaporator. The flow patterns of three fluids of water, ethanol, and 30% glycerol/water solution under the conditions of different tube spacings and two different tube diameters are observed by building a horizontal tube falling film flow experiment platform. Also, four new critical flow patterns are proposed and defined to further clarify the judgment basis of the flow pattern transition. The influence law of different parameters on the flow pattern transition between horizontal tubes is generalized by analyzing the transition mechanism of the flow patterns between tubes. The results of the experiment and analysis show that: The “critical separation length” is the distance sign that there are droplets generating during the process of falling film flow between tubes. That is, the flow patterns are the column flow or the sheet flow when the tube spacing is shorter than the “critical separation length”. The larger the tube spacing, the larger the drop-column transition Re number. At the same time, the growth rate of the critical transition Re number will decrease with the increase of the tube spacing, and the growth rate of the pre-critical transition Re number of the drop-column flow is smaller than the growth rate of the post-critical transition Re number of the drop-column flow. The pre-critical transition Re number of the column-sheet flow does not change significantly with the tube spacing, but the post-critical transition Re number of the column-sheet flow increases with the increase of the tube spacing. The Re number interval of the column-sheet flow is generally larger than that of the drop-column flow at every tube spacing. The tube diameter has no significant effect on the flow pattern transition under the experimental condition. Water and 30% glycerol/water solution show similar critical transition Re numbers, and the critical transition Re number of ethanol is smaller obviously.

Keywords: Horizontal tube falling film flow; Critical flow pattern; Critical separation length

1. Introduction

The heat exchange method of the falling film flow between horizontal tubes has the advantages of high heat exchange efficiency and small heat transfer temperature

difference. Therefore, it is widely used in many fields such as seawater desalination [1], food processing [2], air conditioning and refrigeration [3,4]. Especially it plays an important role in the low temperature multi-effect evaporation (LT-MEE) desalination equipment [5]. As a flow mode for

* Corresponding author.

the purpose of heat transfer, the study of its performance in heat transfer is indispensable. As mentioned in the study by Mu et al. [6] and Chen and Wang [7], the flow patterns between tubes have a decisive effect on the heat and mass transfer performance of the falling film flow. So the study of the flow pattern transition and its influencing factors is of great significance to clarify the mechanism of heat and mass transfer during falling film flow, which helps to control the flow pattern between tubes, and further improve the heat exchange efficiency of the heat exchangers.

Many scholars conduct research on the characteristics of the falling film flow between horizontal tubes and their influencing factors by experimental methods. They also use numerical simulation methods to explore the mechanism as the theoretical support. In terms of experiments, Hu and Jacobi [8] summarize the falling film flow between horizontal tubes into five types, which includes drop flow, drop-column flow, column flow, column-sheet flow, and sheet flow. Wang [9] gives out the method of distinguishing and judging the flow patterns between horizontal tubes, and points out the two intermediate patterns of the drop-column flow and column-sheet flow as the standard for the transition of the flow patterns between tubes. Chen [10] confirms that the spray density is the most important affecting factor of the flow patterns between tubes through experimental research. Shen et al. [11] find that the tube spacing has a great influence on the falling film flow patterns under the same spray density, while the change of the tube diameter within the experimental range has almost no effect on it. Chen [12] carries out a numerical simulation of the falling film flow patterns of water and lithium bromide solution by the software "FLUENT", and obtains the critical transition Re numbers of the three flow patterns including the drop flow, the column flow and the sheet flow. Yao et al. [13] research the flow pattern transition by visualization method under the conditions of 4 working fluids, 4 liquid distribution heights, and 7 liquid distributor specifications, then analyze the influence of the liquid distribution height and the tube spacing on the horizontal tube falling film flow. Sun [14] study the falling film flow process of water and 4 kinds of CaCl_2 solution with different concentrations, and draw the conclusion that the critical transition Re number decreases with the increase of solution concentration. Hao et al. [15], Wang et al. [16] analyze the influence of the initial velocity and the tube spacing on the transition of the falling film flow patterns between the horizontal tubes through their calculation. Roques and Dupont [17] study the flow pattern transition of three fluids (water, ethylene glycol, 50% ethylene glycol/water solution) during the process of the falling film flow outside four different types of tubes. Without considering the effect of the tube spacing, they give a series of flow pattern transition correlations in the form of $\text{Re} = a\text{Ga}^b$, which is used as the judgment criterion for the flow pattern. Zhang [18] explores the formation mechanism of the flow patterns between tubes through experimental research, then analyzes the influencing factors, and finally establishes a flow pattern judgment criterion. Flow visualization of water/ethanol/30% glycerol solution falling in 8/23/38 mm tube spacing is presented by Liu et al. [19], and the process of

droplet flow is illustrated especially. Zhang et al. [20] use lithium bromide solution as the experimental working fluid to study the influence law of the tube spacing and the tube diameter on the flow pattern transition. His results are as follows: when the distance between tubes gradually increases to twice of the original tube spacing, the flow pattern between tubes will become drop flow, and there will be some cross-drop flow in the middle of the horizontal tubes. When the material of the horizontal tube changes from copper to plastic, the flow of the working fluid between tubes shows an oblique phenomenon, the tubes cannot be wetted vertically. Numerical investigation of the evolution and breakup of the liquid film on a structured wall is also carried out by Bender et al. [21].

A large number of scholars have carried out a thorough discussion on the flow patterns of the falling film flow between the horizontal tubes. However, the division of the flow patterns between tubes is not detailed enough. A more precise identification method of the flow patterns should be obtained. In addition, scholars mainly focus on the influence of the relevant parameters on the flow pattern transition, but there is not sufficient research on the formation process and formation mechanism of these flow patterns. In this paper, an experiment platform of falling film flow is established and the high-speed camera technology is used to observe the flow patterns between tubes under different working fluids, different tube spacings, and two different tube diameters. And then the flow pattern transition mechanism between horizontal tubes and its influencing factors are analyzed, which provides the theoretical basis for the design of more efficient horizontal tube falling film heat exchanger.

2. Experimental device and method

2.1. Experimental device

The schematic diagram and the photo of the experimental platform used to observe the flow state of the falling film flow between tubes are shown in Figs. 1 and 2. As shown in Fig. 1, the fluid is pumped to the upper tank from the water storage tank through a pump, and the working fluid flows out from the upper water tank after two baffles. Then the working fluid enters the liquid distributor at a certain flow rate under the control of the regulating valve. The fluid is sprayed to the guide tube and flows down to the test tube under the effect of gravity to achieve a falling film flow. After the working fluid completes the falling film flow, it returns to the storage tank to complete the cycle. There is an overflow plate in the upper water tank, and the overflowing fluid from the overflow plate is directly recovered to the water storage tank. The structure of the baffles and overflow plate in the upper water tank keeps the water level and provides a constant flow rate.

In the experiment, water, 30% glycerol/water solution, and ethanol are used as the working fluids. The critical transition Re numbers of the three fluids under the conditions of two different tube diameters and different tube spacings during the process of the falling film flow are recorded. The tube diameters and tube spacings are shown in Table 1. The tube spacing refers to the center distance of

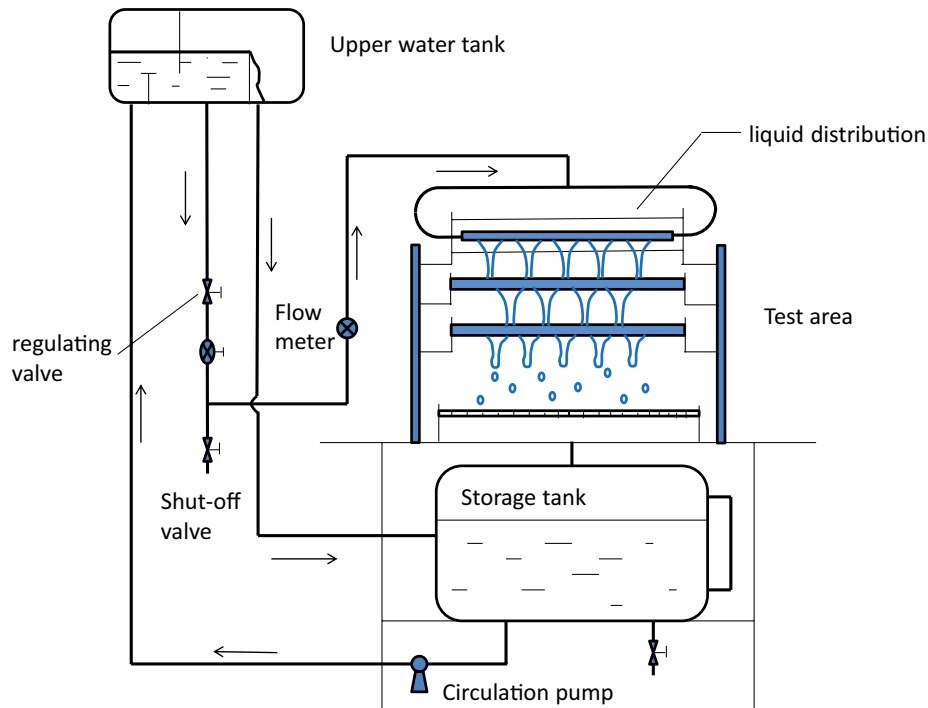


Fig. 1. Schematic diagram of horizontal tube falling film flow circulation system.



Fig. 2. Horizontal tube falling film flow experimental platform.

the upper and lower tubes, which can be precisely adjusted by the slide rail devices on both sides. As shown in Fig. 3, the test tube is installed under the liquid distributor, and its length is 400 mm, the tube diameter has two sizes of 25.4 mm and 19 mm according to the working condition. The test tube is made of aluminum alloy. The experiment is carried out under the normal temperature condition.

The structure of the liquid distribution is shown in Fig. 3. The device is composed of an inner tube (φ 19 mm \times 450 mm), an outer tube (φ 25.4 mm \times 400 mm) and a guide tube (its material and size are the same as the test tube). When the experimental device is working, the working fluid flows in from both ends of the inner tube, overflows through the straight groove at the top of the inner tube, then flows into the gap between the inner and outer tubes, and finally flows out from the hole row at the bottom of the outer tube. Then, the tested fluid is distributed evenly on the test tube through the guide tube, forming a stable and uniform falling film flow. The effective spray length of the liquid distribution device is 300 mm, which is determined by the axial hole-setting length at the bottom of the outer tube.

The image acquisition system uses the backlight shooting method to obtain images with clear boundaries. The backlight shooting method is shown in Fig. 4. LED lights with the power of 100 W provide a stable non-stroboscopic

Table 1
Tube diameter and tube spacing in flow pattern observation

Tube diameter (mm)		Tube spacing (mm)					
19	33.02	38.1	43.18	48.26	53.34	58.42	63.5
25.4	33.02	38.1	43.18	48.26	53.34	58.42	63.5

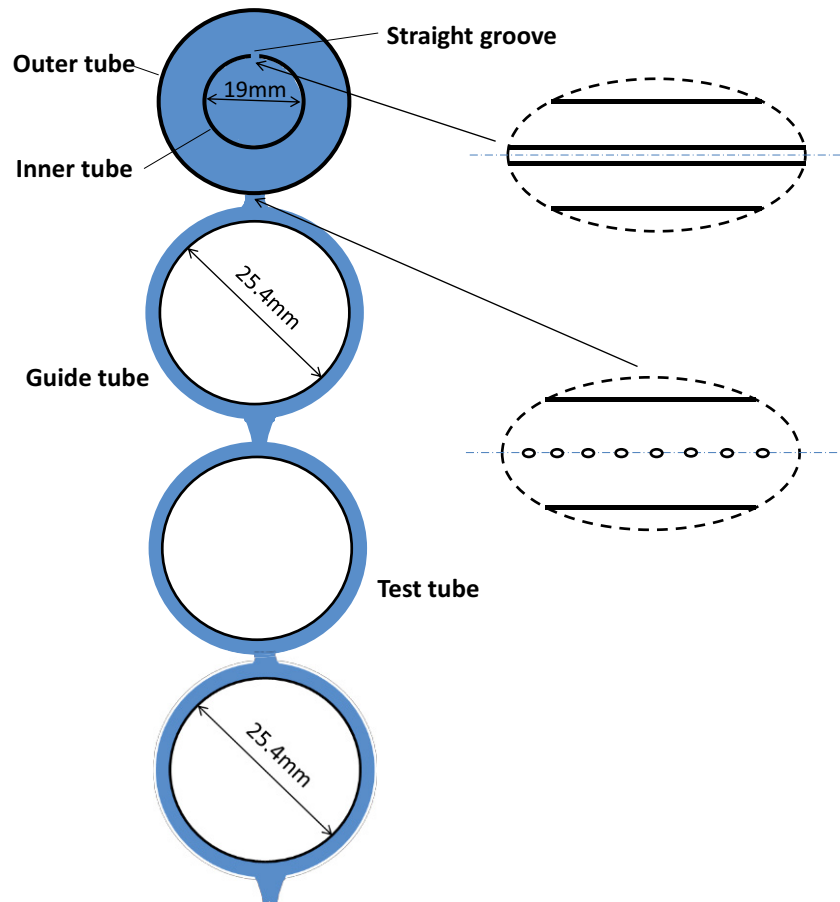


Fig. 3. Schematic diagram of liquid distribution device.

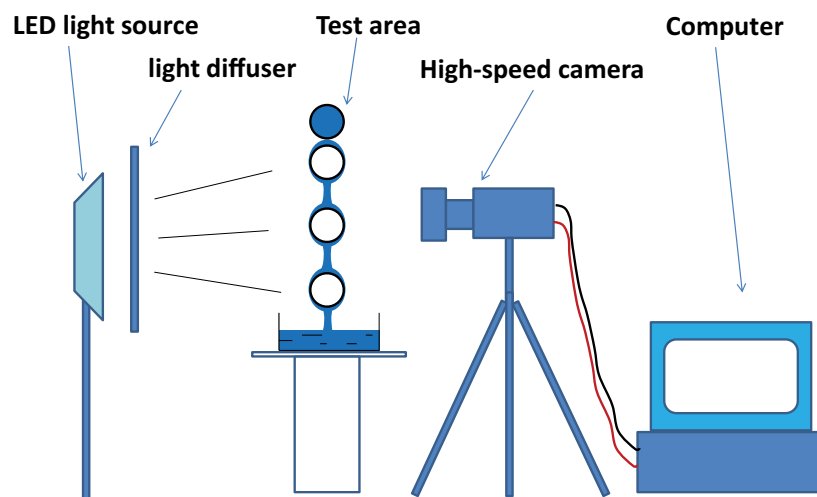


Fig. 4. Schematic diagram of backlit photography.

light source. Light illuminates the experimental area from the back through the light diffuser. The high-speed digital camera Phantom v64.1 is used to photograph the falling film flow pattern of the tested fluid between tubes, and the data is stored in the computer. In the recording process, the frame rate is set to 1,400–2,000 frame/s

according to the actual situation, and the exposure time is set to 60–100 μ s. The image with clear boundaries obtained by the backlight photography method is shown in Fig. 5.

The following table shows the instruments used in the experiment of horizontal tube falling film flow. The relative accuracy and measuring range are listed in Table 2.

The relevant data obtained from the experimental measurement are processed as follows:

- Spray density

According to the measured flow rate in the experiment, it is converted into a single-side spray density in data processing:

$$\Gamma = \frac{G}{2 \times L \times 3,600} \quad (1)$$

where G is the spray amount per unit time, kg/s; L is the effective spray length, m.

- Reynolds number

$$\text{Re} = \frac{4\Gamma}{\mu} \quad (2)$$

where μ is the dynamic viscosity, N·s/m²; Γ is the spray density, kg/m·s; it can be seen that when the physical properties remain constant, the spray density is proportional to Re.

2.2. Experimental error analysis

The experimental error is analysed as follows:

During the experiment, since the spray density Γ cannot be directly measured, it is necessary to indirectly measure

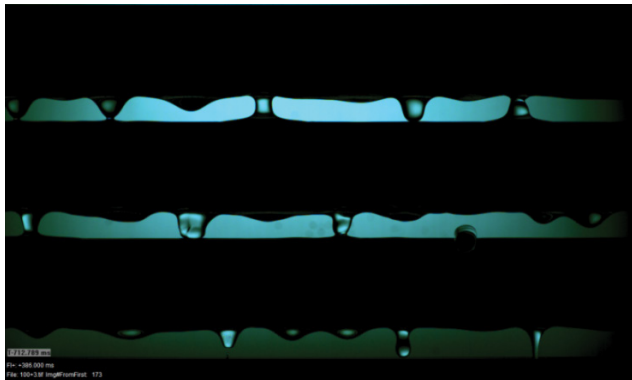


Fig. 5. Flow pattern images obtained by backlit photography.

the parameters G and L , and then calculate Γ from Eq. (1). In the process of obtaining the indirect measured parameters, the measurement error is transmitted, thereby forming the final uncertainty.

Assuming that there is a functional relationship between the required measurement value Y and the indirect measured parameters x_1, x_2, \dots, x_n :

$$Y = f(x_1, x_2, \dots, x_n) \quad (3)$$

The transfer formula of random error is:

$$dY = \left[\left(\frac{\partial f}{\partial x_1} dx_1 \right)^2 + \left(\frac{\partial f}{\partial x_2} dx_2 \right)^2 + \dots + \left(\frac{\partial f}{\partial x_n} dx_n \right)^2 \right]^{\frac{1}{2}} \quad (4)$$

$$\frac{dY}{Y} = \left[\left(\frac{x_1}{Y} \frac{\partial f}{\partial x_1} \frac{dx_1}{x_1} \right)^2 + \left(\frac{x_2}{Y} \frac{\partial f}{\partial x_2} \frac{dx_2}{x_2} \right)^2 + \dots + \left(\frac{x_n}{Y} \frac{\partial f}{\partial x_n} \frac{dx_n}{x_n} \right)^2 \right]^{\frac{1}{2}} \quad (5)$$

For Γ , its uncertainty is:

$$\frac{d\Gamma}{\Gamma} = \left[\left(\frac{dG}{G} \right)^2 + \left(\frac{dL}{L} \right)^2 \right]^{\frac{1}{2}} \quad (6)$$

It can be known from the flow meter that $dG/G = 0.5\%$. Comparing the actual size of the tube with the design size, the processing error is calculated as $dL/L = 1\%$, so:

$$\frac{d\Gamma}{\Gamma} = \left[(0.5\%)^2 + (1\%)^2 \right]^{\frac{1}{2}} = 1.1\% \quad (7)$$

Regard μ as a constant, so:

$$\frac{d\text{Re}}{\text{Re}} = \frac{d\Gamma}{\Gamma} = 1.1\% \quad (8)$$

From the above analysis, the error of the experimental results is 1.1%.

Table 2
List of horizontal tube falling film flow experimental instruments

Name	Model	Precision	Measuring range
Electromagnetic flow meter	–	0.5%	0.01–0.4 m ³ /h
High-speed camera	Phantom V64.1	1,280 pixels × 800 pixels	–
Stopwatch	–	0.01 s	–
Electronic balance	AWH(SA)	0.5 g	0–15 kg
Pressure sensor	DCST-GP	–0.1–0 MPa	0.2 KPa
Pressure gauge	YB150	–0.1–0 Mpa/0–0.1 MPa	0.4 KPa

3. Results and discussion

3.1. Horizontal tube falling film flow pattern and its transition mechanism

3.1.1. Horizontal tube falling film flow pattern

As mentioned above, there are five basic flow patterns of the falling film flow between horizontal tubes, namely: the drop flow, the drop-column flow, the column flow, the column-sheet flow and the sheet flow with the change of spray density from small to large. Taking the working fluid as water, the tube diameter $d = 19$ mm and center distance $s = 58.42$ mm as an example, the flow patterns between tubes are shown in Fig. 6a–e, respectively:

In the experimental research, it is found that the drop-column flow and the column-sheet flow can be further subdivided. Therefore, this paper defines four critical flow patterns: pre-critical drop-column flow, post-critical drop-column flow, pre-critical column-sheet flow, post-critical column-sheet flow. Their definitions and images are as follows:

Pre-critical drop-column flow: as shown in Fig. 7a, the fluid under this flow pattern is sometimes shown in the form of drop flow, and sometimes in the form of drop-column flow. Without changing the experimental conditions, the flow patterns alternately switch randomly over time and do not exist at the same time.

Post-critical drop-column flow: as shown in Fig. 7b, the fluid under this flow pattern is sometimes shown in the form of drop-column flow, and sometimes in the form of column flow. Without changing the experimental conditions, the flow patterns alternately switch randomly over time and do not exist at the same time.

Pre-critical column-sheet flow: as shown in Fig. 7c, the fluid under this flow pattern is sometimes shown in the form of column flow, and sometimes in the form of column-sheet flow. Without changing the experimental conditions, the flow patterns alternately switch randomly over time and do not exist at the same time.

Post-critical column-sheet flow: As shown in Fig. 7d, the fluid under this flow pattern is sometimes shown in the form of column-sheet flow, and sometimes in the form of

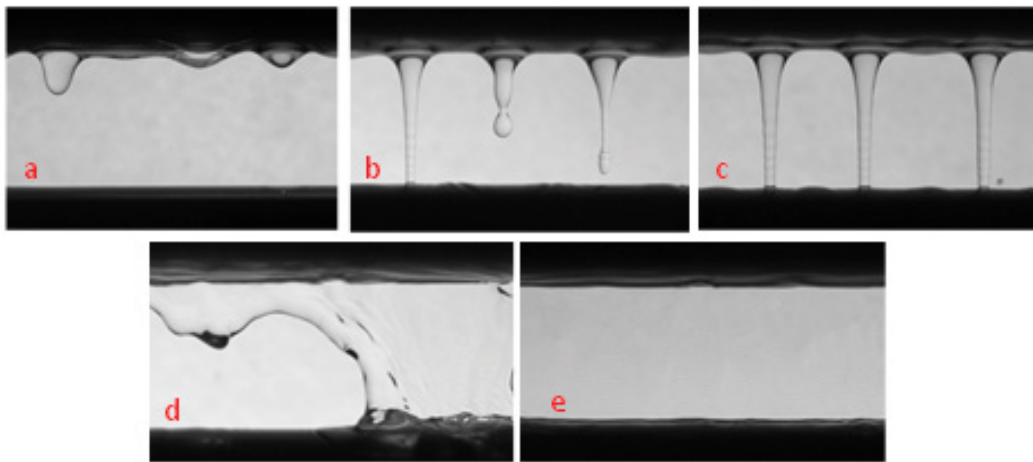


Fig. 6. 5 kinds of flow patterns.

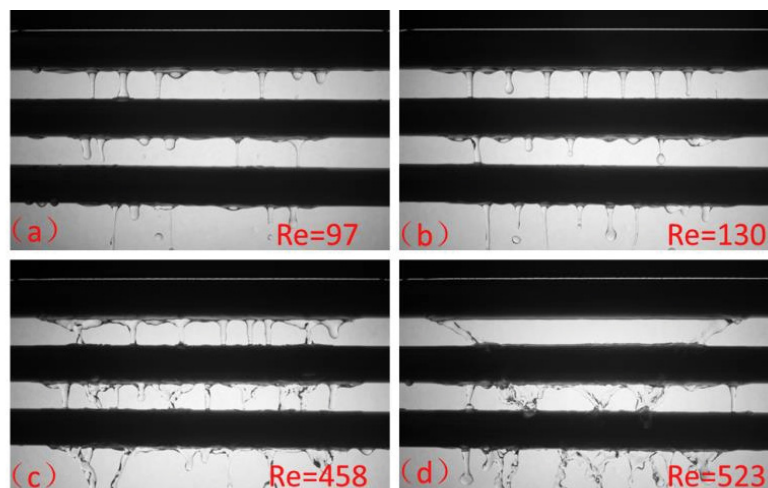


Fig. 7. Critical flow pattern display.

sheet flow. Without changing the experimental conditions, the flow patterns alternately switch randomly over time and do not exist at the same time.

3.1.2. Mechanism analysis of the flow pattern transition between horizontal tubes

3.1.2.1. Mechanism analysis of the drop flow-column flow transition

The complete flow process of a single droplet is shown in Fig. 8. There are four stages during the flow process: droplet formation, droplet falling, droplet impact and the breaking and retraction of the liquid neck. At the same time, the droplet falling process is further divided into three stages, namely the process from the formation of the droplet to the development of the columnar droplet, the process of the columnar droplet developing into a main droplet with a liquid neck and finally leaving the liquid neck, and the process of the separating droplet falling until it touches the surface of the lower tube.

In the second-stage, the main body of the columnar droplet falls downward due to the effect of the gravity, and the upper liquid adheres to the bottom of the tube under the effect of the viscous force and the surface tension, causing the neck of the columnar droplet to be stretched and contracted. And the smaller the diameter of the liquid neck, the greater the surface tension it bears, which promotes the liquid neck to shrink further until it is pinched off, resulting in droplet separation. The distance from the separation point to the bottom of the upper tube is defined as the critical separation length d_c . The critical separation length d_c increases with the increase of the flow rate in the interval of the drop flow. The continuously falling liquid replenishes the liquid neck with the further increase of the flow rate. The liquid neck gets more fluid supply to maintain its diameter during the stretching process so as not to be pinched off, which greatly delays the separation of the droplet from the liquid neck and further increases the critical separation length. At the same time, the flow replenishment process causes more liquid to accumulate in the liquid neck, which makes the liquid neck more stable. The effect of surface tension is weakened, and the retraction process of the liquid neck at this time. Instead, due to the Prado-Rayleigh instability, nodules appear at the end of the liquid neck after the first droplet separation. And a continuous and stable droplet separation process will continue for a period of time at the end of the liquid neck (as

shown in Fig. 9). Therefore, the condition for the generation of droplets is that the tube spacing is longer than the critical separation length. When the tube spacing is shorter than the critical separation length, no droplets will be generated, and the flow between tubes appears as the column flow pattern.

When the liquid arrives at the bottom of the upper tube, a horizontal spreading process occurs while the liquid gathers and falls vertically. The horizontal flow causes the liquids to mix and pull each other under the effect of surface tension. This leads to the instability of the flow between tubes, resulting in uneven flow distribution at different dripping points, which further leads to the difference in the critical separation length at different dripping points. The flow pattern between tubes is shown as a drop-column flow when the critical separation lengths at some dripping points are longer than the tube spacing, and the critical separation lengths at other dripping points are shorter than the tube spacing (as shown in Fig. 10). As mentioned above, the stable droplet separation process continues after the first droplet separation. However, the

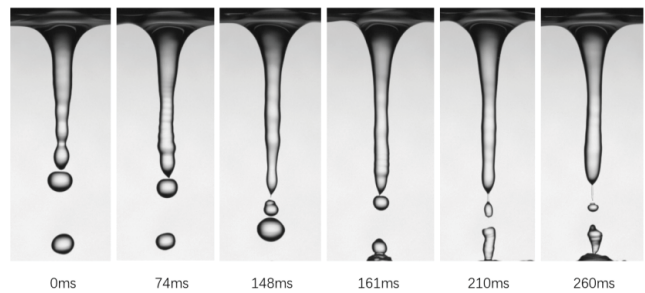


Fig. 9. Continuous droplet separation process.



Fig. 10. Drop-column flow pattern.

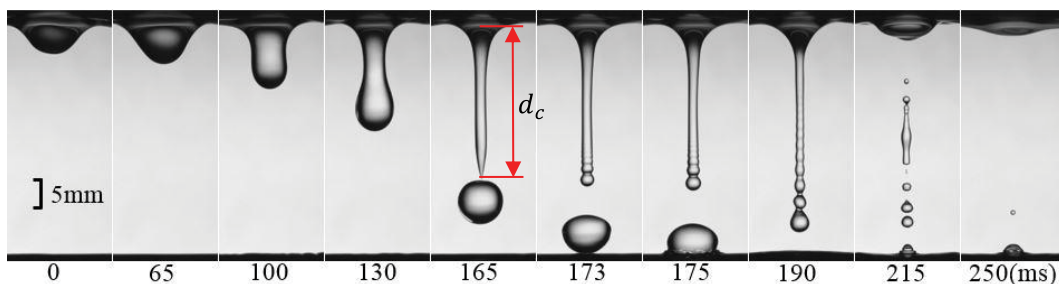


Fig. 8. Generation process of the droplet.

stability of the separation process is relative and time-sensitive. The flow rate of the same dripping point changes over time due to the instability, resulting in the change in the separation length. This is also one of the formation mechanisms of the drop-column flow pattern.

3.1.2.2. The analysis of the drop-column transition mechanism

Fig. 11a shows a complete flow unit of the column flow. It can be found from the observation of the column flow pattern that there is a “liquid valley” in the middle of the adjacent liquid column at the bottom of the upper tube. This is because the liquid horizontally spreads while gathering and falling at the bottom of the upper tube. The horizontally flowing liquid converges at the middle position of the adjacent liquid column, thereby forming the liquid valley, and the liquid valley remains stable under the effect of surface tension and gravity.

When the flow rate increases, the flow pattern between tubes is shown in Fig. 11b, and the column flow pattern becomes unstable at this time. The mass of the fluid entering the “liquid valley” is greater than the mass that the adjacent liquid column can attract and carry away, which cause

the liquid to gather at the valley, then overcome the surface tension and begin to fall. The droplet takes away part of the liquid in the valley during the falling process, and the liquid mass at the root of the liquid valley decreases. The falling liquid begins to shift towards the adjacent liquid column under the effect of the surface tension. The liquid neck begins to fuse with the adjacent liquid column after the droplet separates from the liquid neck, and the liquid root connection is formed at the bottom of the upper tube. The liquid root connection is the initial stage of the transition from column flow to sheet flow.

As shown in Fig. 12, the flow rate of the horizontal flow at the bottom of the upper tube increases as the flow rate further increases, and the liquid mass in the flow unit also greatly increases. At the same time, the falling process of the liquid between the adjacent liquid columns at the bottom of the upper tube will be supplemented by sufficient working liquid, so that the liquids fuse with each other, then the adjacent liquid columns on both sides overcome the inertial force to converge and fuse to the middle under the effect of surface tension, forming a complete partial sheet flow area A. At this time, there are still independent liquid columns that have not been connected

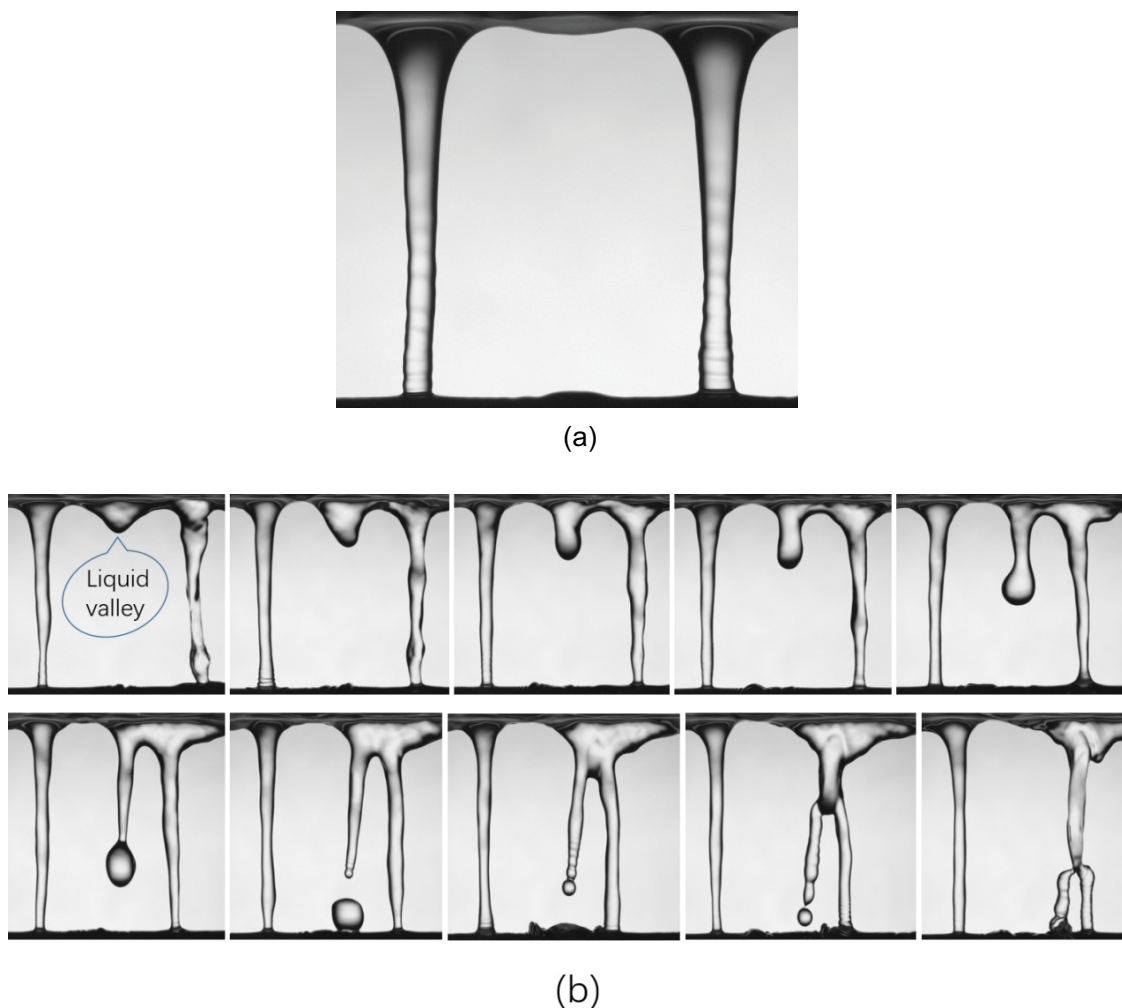


Fig. 11. Initial stage of the transition from column flow to sheet flow.

or merged outside the partial liquid sheet, so the flow pattern between tubes appears as the column-sheet flow state. Obviously, under this mechanism, the liquid column between tubes and the partial liquid sheet will continue to merge to form a larger area of the liquid sheet as the flow rate further increases until the whole target area is covered. And the flow pattern will be converted to sheet flow.

3.2. Influence of the tube spacing on flow pattern transition

The four newly defined flow patterns are used in this paper to reflect the critical interval of the flow pattern transition of the falling film flow between the horizontal tube, thereby to conduct a more detailed quantitative analysis of the factors affecting the flow state between tubes.

Fig. 13 shows the distribution law of the critical transition Re number of 4 flow patterns between tubes with the working fluid of pure water and the tube diameter of 19 mm under different tube spacings. When $s = 33.02$ mm, the distance between tubes is too small, leading to flow phenomena such as “fake column”. It is difficult to define the flow pattern between tubes, and there is a large observation error, so the results under the condition of $s = 33.02$ mm are not analyzed in this paper. It can be seen that the transition Re numbers of the critical flow patterns generally show an upward trend in the process of increasing the tube spacing from $s = 38.1$ mm to $s = 63.5$ mm.

It can be seen from the previous analysis of the drop-column transition mechanism that the critical separation length is the key parameter of drop-column transition. The critical separation length increases with the increase of the flow rate until it is equal to the distance between tubes, which is the sign of the drop-column transition. Therefore, the greater the tube spacing, the greater

the separation length corresponding to the drop-column transition (including both the pre-critical and the post-critical of the drop-column flow), and the greater the flow rate required. At the same time, it can be seen from the figure that the growth rate of the pre-critical and the post-critical transition Re number of the drop-column flow decreases with the increase of the tube spacing. Analyzing the change law of the critical separation length with the increase of the flow rate (Fig. 14), it can be concluded that the critical separation length growth rate increases as the Re number increases. Conversely, this phenomenon causes that the growth rate of the required flow decreases as the separation length increases, that is, the

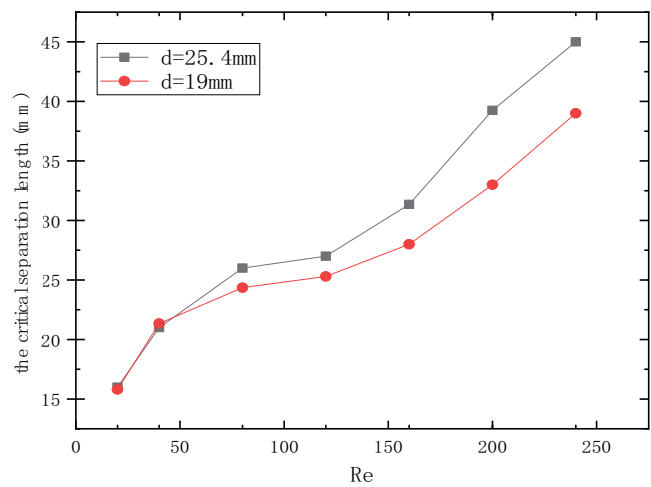


Fig. 14. Change law of the critical separation length with the increase of the flow rate.

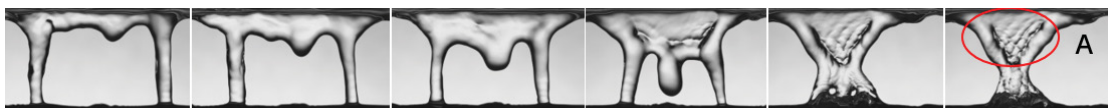


Fig. 12. Transition from column flow to sheet flow as the flow rate increases.

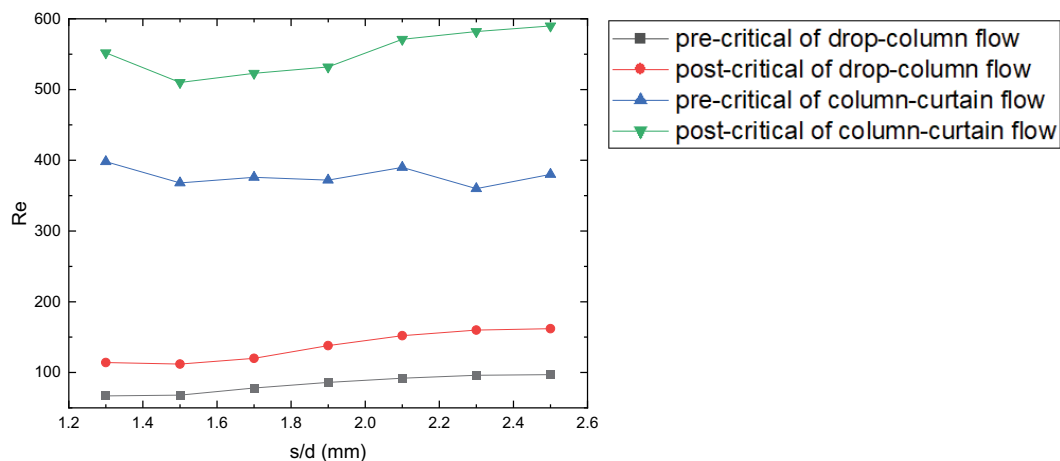


Fig. 13. Distribution of the critical points of the four flow regimes at different tube spacings.

growth rate of the pre-critical and the post-critical transition Re number of the drop-column flow decreases as the tube spacing increases. It can be seen from the foregoing that flow instability is an important cause of the drop-column flow. Flow instability makes the flow distribution uneven, which causes some droplet generation points to get more liquid for a certain period of time, so that the separation length exceeds the distance between tubes to form a liquid column, which promotes the formation of the pre-critical of the drop-column flow. More liquid columns will be formed as the flow rate increases. At this time, the uneven flow distribution caused by flow instability will become an obstacle to the transition from the drop-column flow to the column flow. A larger flow supply is required to overcome the flow instability and completely transform the flow pattern into the column flow. Therefore, as shown in Fig. 13, while the flow rate required for the drop-column transition increases with the increase of the tube spacing, the flow instability intensifies, which promotes the formation of the pre-critical of the drop-column flow and hinders the formation of the post-critical of the drop-column flow. This makes the pre-critical transition Re number of the drop-column flow increase more slowly than the post-critical transition Re number of the drop-column flow. This also makes the flow interval corresponding to the drop-column flow increase when the tube spacing increases.

During the process of the column-sheet transition, it can be known from the column-sheet transition mechanism that, similar to the drop-column transition, the area of the liquid sheet between tubes and the required flow rate increase with the increase of the tube spacing. At the same time, the increased flow instability further hinders the formation of liquid sheet, which makes the transition Re number show an upward trend. However, it is worth noting that this trend is only reflected in the post-critical pattern of the column-sheet flow, and the Re number corresponding to the pre-critical pattern of the column-sheet flow does not change significantly with the tube spacing. The early stage of the column-sheet transformation is actually a process in which liquid gathers and falls at the “liquid valley”, and generates the root connection at the bottom of the upper tube. This process occurs at the bottom of the upper tube and is not affected by the lower tube. Therefore, the pre-critical transition Re number of the column-sheet flow does not change significantly with the tube spacing.

It can be seen from Fig. 13 that the Re number interval of the column-sheet transition is generally larger than that of the drop-column transition at every tube spacing. This is because the energy required to resist the rupture of the liquid sheet when the column-sheet flow changes its flow pattern is greater than the energy required to resist the breakage of the liquid column when the drop-column flow changes its flow pattern. At the same time, the flow supplement required for connecting the liquid columns to form the liquid sheet during the process of the column-sheet transition is far greater than the flow supplement required for the drop-column transition, so the flow range of the column-sheet transition process is larger than that of the drop-column transition process.

3.3. Influence of the tube diameter on flow pattern transition

Fig. 15 shows the critical transition Re number when pure water flows between tubes under the conditions of the tube spacing $s = 48.26$ mm and respectively tube diameters $d = 19$ mm and $d = 25.4$ mm. It can be seen from Fig. 15 that there is little difference in the flow pattern transition curve under the conditions of two different tube diameters. The pre-critical and post-critical transition Re number under the condition of tube diameter $d = 19$ mm is approximately the same as that under the condition of tube diameter $d = 25.4$ mm. The influence of tube diameter on the transition of flow patterns between tubes is not obvious. However, it can be seen from the analysis that the difference in tube diameter is mainly reflected in the curvature of the tube wall. Curvatures will not only affect the flow speed of the liquid film outside the tube, but also affect the formation of the liquid film on the tube wall. The larger the tube diameter, the greater the curvature of the tube, the greater the impact on the gather and fracture of the liquid film at the bottom of the tube. So theoretically, the difference in tube diameter will affect the flow pattern between tubes. In view of this, we take the drop-column transition as an example to compare the law of the critical separation length changing with the flow rate under two different tube diameters (as shown in Fig. 16), so as to analyze the influence of the tube diameter on the flow patterns between tubes. The horizontal line in Fig. 16 shows the distance between tubes under the condition of $s = 48.26$ mm. It can be seen that when the separation length reaches this distance, the corresponding Re numbers under the two different tube diameters are very close. However, it can be found from the figure that as the flow rate increases, the growth rate of the critical separation length under the condition of tube diameter $d = 25.4$ mm is greater than that under the condition of tube diameter $d = 19$ mm. Therefore, it is reasonable to predict that as the pipe spacing increases, that is, when

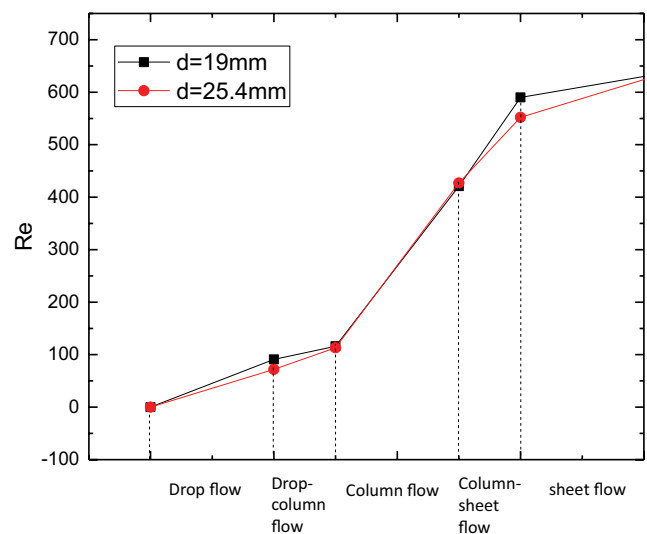


Fig. 15. Critical Re of fluid state transition under two different tube diameters.

the separation length required for the drop-column transition continues to increase (as shown by the lines b and c), The critical transition Re number under the condition of tube diameter $d = 25.4$ mm will be smaller than that under the condition of tube diameter $d = 19$ mm. In summary, when $s = 48.26$ mm, there is no obvious difference in the flow pattern transition process when pure water flows under the different conditions of tube diameter $d = 19$ mm and $d = 25.4$ mm. However, the influence of the tube diameter on the transition of the flow pattern will become apparent as the tube spacing increases.

3.4. Influence of the working fluid on flow pattern transition

Fig. 17 shows the critical transition Re number for three different working fluids under the conditions of tube diameter $d = 25.4$ mm and tube spacing $s = 43.18$ mm. It can be seen that the critical transition Re number of water is not

much different from the critical transition Re number of 30% glycerol. There is a 14% difference in pre-critical transition Re number of drop-column flow and a 6% difference in post-critical transition Re number. There is a 3% difference in pre-critical transition Re number of column-curtain flow and a 4% difference in post-critical transition Re number. The critical transition Re number of ethanol is significantly lower than that of 30% glycerol and water.

The critical separation length is an important parameter in studying the drop-column transition process. And it can be seen from the analysis of Table 3 that the surface tension of the liquid is the main physical parameter which affects the difference in the critical separation length during the process of the falling film flow between horizontal tubes. The critical separation length is actually the limit length that the liquid neck can maintain without breaking, and the process of liquid neck rupture is precisely the process of being pinched off by the surface tension of the liquid. The smaller the surface tension of the liquid is, the less easily the liquid neck is to be pinched off, and the longer it can stretch. The surface tension of ethanol is much smaller than that of water, so its critical separation length is much larger than that of water at the same flow rate. This is consistent with experimental measurements (as shown in Fig. 18). Fig. 18 shows that critical separation length of ethanol is much longer than that of water under the same Re number. Therefore, when the tube spacing is the same, that is, the critical separation length

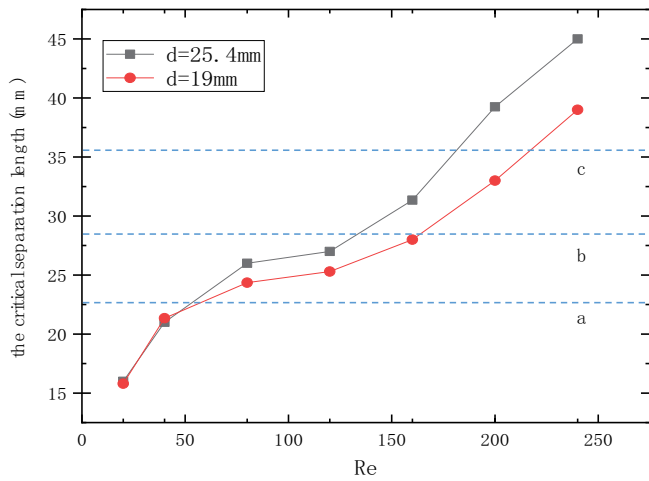


Fig. 16. Law of the critical separation length changing with the flow rate under two different tube diameters.

Table 3
Physical properties of different working fluids

Working fluid	Dynamic viscosity (Pa·s)	Surface tension (N/m)
Water	0.001004	0.072
30% glycerol	0.00264	0.0633
Ethanol	0.001074	0.02197

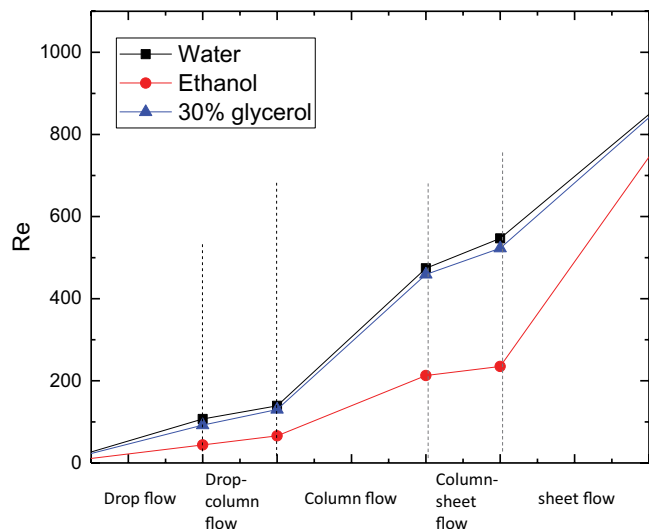


Fig. 17. Flow state transition critical Re under different physical properties.

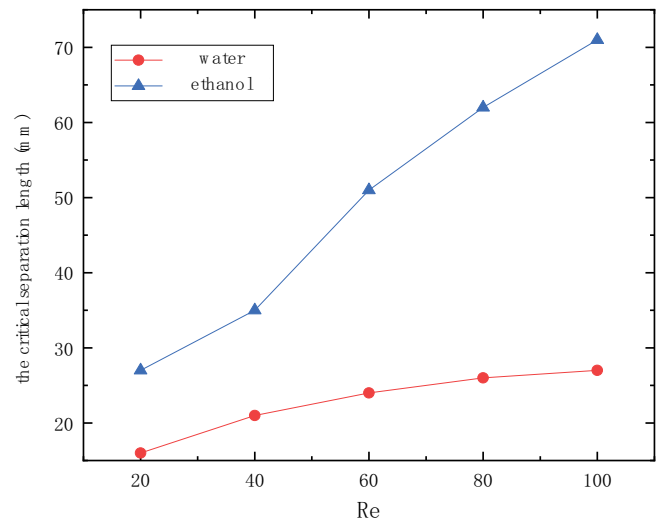


Fig. 18. Comparison of the change law of critical separation length between pure water and ethanol.

required for the transition is the same, the flow rate of ethanol is much smaller than that of water.

There are two important stages during the process of the column-curtain transition, one is the gathering and falling of liquid in the liquid valley, and the other is the connection and the liquid sheet formation of the falling liquid. The process of liquid gathering and falling in the liquid valley is actually a droplet generation process. As the flow rate increases, the liquid continues to gather in the liquid valley until it reaches the “escape length” and starts to fall. Liu elaborates on the formation mechanism of the droplets at the bottom of the upper tube, and points out that it is essentially a process of gravity and surface tension opposing each other. The surface tension makes the droplets adhere to the bottom of the upper tube and cannot fall when the flow rate is small. More liquid enters the droplet under the induction of gravity as the flow rate increases. The diameter of the droplet grows slowly under the constraint of surface tension until the droplet reaches a critical volume. The droplet will become unstable when it exceeds the critical volume. The surface tension is not enough to resist the gravity of the droplet, so the droplet size grows rapidly and the droplet starts to fall. This critical size is the “escape length”. It can be seen from Table 3 that the surface tension of ethanol is much smaller than that of water, so the “escape length” of ethanol is much smaller than that of water, and the required flow rate when there are droplets generating at the bottom of the upper tube and the corresponding transition Re numbers during the column-sheet transition are both smaller than water. At the same time, surface tension is a kind of surface contraction force acting on the surface of the fluid, which makes the fluid try to maintain its original flow state. Therefore, the surface tension hinders the formation of the liquid film in the subsequent connection and film formation process of the working fluid. The surface tension of alcohol is smaller than that of water, so this kind of obstruction is also smaller, the flow pattern between tubes is more easily transformed into the sheet flow.

In addition, it was found during the experiment that, compared with water and 30% glycerol, ethanol has a faster drop breaking speed and a higher dripping frequency in the range of drop flow. This is because ethanol has a small surface tension, which causes its flow pattern easily affected and broken.

4. Conclusion

In this paper, a falling film flow between horizontal tubes experiment is carried out. By processing the pictures taken by a high-speed camera, the transition Re number of the critical flow pattern is calculated, and the different performance of the flow pattern under different conditions is observed and analyzed. Conclusions can be drawn as follows by comparing the transition Re numbers of the critical patterns under the conditions of different fluid physical properties (water, 30% glycerol, ethanol), two different tube diameters ($d = 25.4$ mm, $d = 19.04$ mm) and different tube spacings ($s = 33.02, 38.1, 43.18, 48.26, 53.34, 58.42, \text{ and } 63.5$ mm):

- Four new critical flow patterns are defined: pre-critical drop-column flow, post-critical drop-column flow,

pre-critical column-curtain flow, post-critical column-curtain flow. The transition process of falling film flow between tubes is studied and divided in more detail.

- The critical separation length is the distance sign of the generation of droplets between tubes. When the tube spacing is shorter than the critical separation length, no droplets will be generated, and the flow between tubes appears as the column flow pattern. At the same time, the flow instability leads to uneven flow distribution at the bottom of the upper tube, which results in the formation of the drop-column flow.
- The column-sheet transition process is divided into two important stages. In the first stage, the liquid accumulates in the “liquid valley” until the gravity exceeds the surface tension, then the droplet reaches the “escape size” and falls. In the second-stage, the liquid merges with the adjacent liquid columns under the effect of surface tension during the falling process. As the flow rate increases, the connection area continues to expand until the liquid sheet eventually covers the target area, and the flow pattern between tubes is converted to the sheet flow.
- The greater the tube spacing, the greater the critical transition Re number corresponding to the drop-column transition (including both the pre-critical and the post-critical of the drop-column flow). And the growth rate of the pre-critical and the post-critical transition Re number of the drop-column flow decreases as the tube spacing increases. At the same time, while the flow rate required for the drop-column transition increases with the increase of the tube spacing, the flow instability intensifies, which promotes the formation of the pre-critical of the drop-column flow and hinders the formation of the post-critical of the drop-column flow. This makes the pre-critical transition Re number of the drop-column flow increase more slowly than the post-critical transition Re number of the drop-column flow. This also makes the flow interval corresponding to the drop-column flow increase when the tube spacing increases. The post-critical transition Re number of the column-sheet flow increases with the increase of the tube spacing, but the pre-critical transition Re number of the column-sheet flow does not change significantly with the tube spacing. The Re number interval of the column-sheet transition is generally larger than that of the drop-column transition at every tube spacing.
- Theoretically, the difference in the tube diameter can affect the flow pattern between tubes. But when $s = 48.26$ mm, there is no obvious difference in the flow pattern transition process when pure water flows under the different conditions of tube diameter $d = 19$ mm and $d = 25.4$ mm.
- The surface tension of the liquid is the main physical parameter that affects the flow pattern transition under the conditions of the same spray density and different working fluid. It is concluded that the critical transition Re numbers of water and 30% glycerol are similar and the critical transition Re number of ethanol is significantly lower than that of 30% glycerol and water under the experimental conditions of this article.

Acknowledgment

The research is supported by the Project of National Natural Science Foundation of China (No.52076027, 51936002), and the Fundamental Research Funds for the Central Universities (No.DUT19LAB19).

References

- [1] A.D. Khawaji, I.K. Kutubkhanah, J.-M. Wie, Advances in seawater desalination technologies, *Desalination*, 221 (2008) 47–69.
- [2] G. Ribatski, A.M. Jacobi, Falling-film evaporation on horizontal tubes—a critical review, *Int. J. Refrig.*, 28 (2005) 635–653.
- [3] J. Fernández-Seara, Á.Á. Pardiñas, Refrigerant falling film evaporation review: description, fluid dynamics and heat transfer, *Appl. Therm. Eng.*, 64 (2014) 155–171.
- [4] M.G. He, X.F. Wang, Y. Zhang, Review of prior research and new technology for horizontal-tube falling-film evaporator used in refrigeration, *J. Chem. Ind. Eng. (China)*, 59 (2008) 23–28.
- [5] S.Q. Shen, G.T. Liang, Distribution of heat transfer coefficient in horizontal-tube falling film evaporator, *CIESC J.*, 62 (2011) 3381–3385.
- [6] X. Mu, S. Shen, Y. Yang, G. Liang, X. Chen, J. Zhang, Experimental study on overall heat transfer coefficient of seawater on three tube arrangements for horizontal-tube falling film evaporator, *Desal. Water Treat.*, 57 (2016) 9993–10002.
- [7] Z.G. Chen, S.F. Wang, Numerical simulation and experimental study on heat transfer performance of falling film outside the horizontal tube, *Chem. Eng. Mach.*, 45 (2018) 757–763.
- [8] X. Hu, A.M. Jacobi, The intertube falling film: part 1—flow characteristics, mode transitions, and hysteresis, *Heat Transfer*, 118 (1996) 616–625.
- [9] Z. Wang, Experimental Study on the Dynamics of Falling Film of Horizontal Tube Bundle and the Interface Absorption Performance, Tianjin University, China, 2008.
- [10] X. Chen, Flow and Evaporation Heat Transfer of Seawater Falling-Film around Horizontal Tube, Dalian University of Technology, China, 2015.
- [11] S.Q. Shen, X. Chen, X.S. Mu, The effect of tube spacing on flow pattern and heat transfer of horizontal tube falling film evaporation, *J. Harbin Eng. Univ.*, (2014) 1492–1496.
- [12] J.D. Chen, Numerical Simulation and Experimental Research on Flow Pattern of Falling Film between Horizontal Tube, Beijing University of Civil Engineering and Architecture, China, 2014.
- [13] N. Yao, A. Wu, J. Lin, Experimental study on flow pattern conversion between horizontal tubes falling-film evaporator, *Refrig. Air-conditioning*, 20 (2020) 54–58.
- [14] W.Q. Sun, Experimental Research and Numerical Simulation of Falling Film Flow Process Outside Horizontal Tube, Graduate University of Chinese Academy of Sciences, China, 2013.
- [15] H. Hao, B.I. Qincheng, Z. Xiaolan, Numerical study on flow and heat transfer characteristics of horizontal-tube falling-film evaporators in seawater desalination system, *Proc. CSEE*, 31 (2011) 81–87.
- [16] X.F. Wang, M.G. He, Y. Zhang, Numerical simulation of the liquid flowing outside the tube of the horizontal-tube falling film evaporator, *J. Eng. Thermophys.*, 29 (2008) 1347–1350.
- [17] J.F. Roques, V. Dupont, Falling film transitions on plain and enhanced tubes, *J. Heat Transf.*, 124 (2002) 491–499.
- [18] D. Zhang, Research on Flow Pattern and Two-phase Flow Characteristics between Horizontal Tube Falling Film Evaporator Tubes, Yanshan University, China, 2020.
- [19] S.L. Liu, S.Q. Shen, X.S. Mu, Y. Guo, D.Y. Yuan, Experimental study on droplet flow of falling film between horizontal tubes, *Int. J. Multiphase Flow*, 118 (2019) 10–22.
- [20] R.H. Zhang, J.D. Chen, R.P. Niu, Experimental research on the factors affecting the flow pattern of the falling film flow between horizontal tubes, *Sci. Technol. Eng.*, 16 (2016) 43–47.
- [21] A. Bender, P. Stephan, T. Gambaryan-Roisman, Numerical investigation of the evolution and breakup of an evaporating liquid film on a structured wall, *Int. J. Heat Fluid Flow*, 70 (2018) 104–113.